A theoretical study on the performance of a scroll expander in an organic Rankine cycle with hydrofluoroolefins (HFOs) in place of R245fa

Antonio Giuffrida

Politecnico di Milano — Dipartimento di Energia, Via R. Lambruschini 4, 20156, Milano, Italy

Global warming is the leading environmental concern of the 21st century, promoting active areas of research as the development of low global warming potential (GWP) refrigerants such as hydro-fluoroolefins (HFOs).

This work investigates the performance of a 2 kW hermetic scroll expander by means of a semi-empirical model when replacing the original working fluid (R245fa) with low-GWP fluids. Calculation results of micro organic Rankine cycle (ORC) systems are presented, after setting the power output from the expander, and the relation between cycle efficiency and maximum cycle temperature is reported for seven selected fluids. In detail, almost equal performance of R1234ze(Z) compared to R245fa and slightly better performance when using R1224yd(Z) or R1233zd(E) are achieved, even though a modest increase of the fluid temperature at the expander inlet is necessary for the last two fluids. In case of lower heat sources, R1234yf, R1243zf and R1234ze(E) are indicated as working fluids and mixtures of HFOs are also considered to extend the operation range of the expander. On the other hand, limited to this case study, R1336mzz(Z) does not seem to be an interesting fluid, because of the calculated higher temperature at the expander inlet and lower expander efficiency.

Keywords:
Organic Rankine cycle
R1234ze(Z)
R1224yd(Z)
R1233zd(E)
R1336mzz(Z)
Scroll expander

1. Introduction

The organic Rankine cycle (ORC) is a technology for mechanical energy production with growing interest in the last years due to its potential integration in distributed generation systems and its favorable characteristics to exploit low-temperature heat sources [1]. One of the main advantages is the possibility of matching the ORC operation to the heat source and heat sink characteristics by means of the selection of the working fluid among a considerable set of substances [2,3]. In detail, ORC systems are successfully used in several geothermal and biomass-fired power plants, but there is also a great interest in ORC utilization to exploit waste heat and exhaust gases of combustion turbines and reciprocating engines as well as solar thermal energy [4].

As a core component of the ORC system, the expander has a vital role in the overall system performance. In general, expanders can be categorized into two types: the first is the dynamic type, such as the axial-flow turbine; the second is the volumetric type, such as the scroll expander. Currently, expanders with kW scales are under development and demonstration. As a matter of fact, several types of commercial scroll machines can be modified into expanders and integrated into ORC systems for low grade heat recovery. In particular, a number of researchers [5] have investigated the performance of scroll expanders resulting from original hermetic refrigeration compressors, automotive air-conditioning compressors and open-drive scroll air compressors. Paying attention to the technical literature about ORC systems with scroll-type expanders, R123, R134a and R245fa are the most investigated working fluids, based on both theoretical and experimental approaches [5–9]. Nevertheless, it should be considered that R123 belongs to the hydrochlorofluorocarbon (HCFC) family, with a non-zero ozone depletion potential (ODP), whereas R134a and R245fa are hydrofluorocarbons (HFCs), the so-called third generation refrigerants with no effect on the ozone layer. Although HFCs are currently dominating the refrigerant market, they have a high global warming potential (GWP). For instance, the widely used R245fa has a GWP of 858 [10]. After the global phase-out of chlorofluorocarbons (CFCs) and hydrochlorofluorocarbons (HCFCs), governments are now aiming at phasing down the emissions of

E-mail address: antonio.giuffrida@polimi.it.

Published Journal Article available at: https://doi.org/10.1016/j.energy.2018.07.146

hydrofluorocarbons (HFCs), by also including them into the regulatory regime of the Montreal Protocol. Hence a key question is what alternatives will replace HFCs.

1.1. Hydrofluorolefins as low-GWP fluids

Recent research and development activity is focusing on hydrofluoroolefins (HFOs), i.e. fluorinated propene (propylene) isomers, as potential working fluids with low GWP. As an example, referring to European regulations regarding automotive applications, R1234yf is considered to be an excellent drop-in replacement for the conventional R134a [11]. Indeed, some automotive manufacturers in Europe are planning to gradually adopt R1234yf as the main refrigerant for the air conditioning system.

As hydrofluoroolefins such as R1234yf and even R1234ze(E) have started to replace R134a in vapour compression systems [12,13], the potential of these fluids for ORC applications has gained interest. Liu et al. [14] theoretically investigated eight HFOs and found promising results in terms of system efficiency, especially for low-to-medium temperature geothermal ORC power generation. Le et al. [15] optimized both non-regenerative and regenerative su-percritical ORC systems for a low-temperature heat source fixed at 150 °C with interesting results for R1234ze(E). On the other hand, R1234yf is not suggested to be a preferable fluid for ORC applica-tions in terms of thermal efficiency at least for low-to-medium temperature heat sources [16]. Petr and Raabe [17] numerically evaluated R1234ze(Z) as drop-in replacement of R245fa for ORC applications with heat sources in the range of 100−250 °C by means of a simplified cycle model. They concluded that for tem-peratures above 224 °C, R1234ze(Z) showed a slightly higher net power but the performance was in line with R245fa for the majority of the range of heat source temperatures considered. R1234ze(Z) was also considered by Ziviani et al. [18], with performance results comparable to R245fa, in line with the research of Petr and Raabe [17]. Two other low-GWP working fluids, namely R1233zd(E)[1] and R1336mzz(Z), were studied by Moles et al. [19], who compared the predicted ORC performance over a wide range of evaporating temperatures, condensing temperatures and degrees of vapor superheating. Both the fluids would enable higher net cycle effi-ciency than R245fa, even though the cycle with R1336mzz(Z) is benefitted substantially by a recuperator. Experimental in-vestigations on these two fluids were also carried out by the same authors [20,21]. Another experimental study on R1233zd(E) as a drop-in replacement for R245fa in ORC systems was also proposed by Eyerer et al. [22]: in addition to the advantage of a much smaller GWP, using R1233zd(E) involves higher thermal efficiency.

1.2. Objective of the paper

The number of research papers reported above highlights the interest in HFO as low-GWP fluids for ORC applications. This paper is a revised and extended version of an earlier conference paper [23] focusing on a 2 kW hermetic scroll expander for use in a micro-scale Rankine cycle, originally operating in a system with R245fa. This work aims at simulating the performance of the scroll expander in case of replacing the original R245fa with HFOs as possible alternative fluids. In detail, the next section deals with (i) the semi-empirical model for the simulation of the scroll machine, as formerly reported by Lemort et al. [24], and (ii) the procedure originally proposed by the author [25] for a reasonable assessment of the performance in case of other working fluids. Ultimately, the results of the performance simulations are presented in terms of power output and efficiency of the micro ORC system equipped with the considered expander.

[1] More precisely this fluid is an hydrochlorofluoroolefin (HCFO), as a chlorine atom is present in the molecule.

2. Modelling the scroll expander

This section details the semi-empirical model for the simulation of the scroll expander [24] and the procedure originally proposed in a former work [25] for a reasonable assessment of the performance in case of different working fluids.

2.1. The semi-empirical model

The scroll expander dealt with in the current work is the one previously investigated by Lemort et al. [24], who proposed a semi-empirical model to simulate the performance of the scroll machine in case of R245fa as the working fluid. For the sake of brevity, only the main features of the modelling approach are recalled here, but further specific details can be found elsewhere [26].

As schematized in Fig. 1, the evolution of the working fluid through the expander is decomposed into a number of consecutive steps:

- an adiabatic pressure drop (su → su,1),
- an isobaric cooling down by contact with the metal mass of the machine (su,1 → su,2) during the intake process,
- a first isentropic expansion of the flow rate $\dot{m}_{in}$ down to the adapted pressure imposed by the built-in volume ratio (BVR) of the machine (su,2 → ad),
- a second adiabatic expansion of the flow rate $\dot{m}_{in}$ at constant machine volume (ad → ex,2),
- a throttling of the leakage flow rate $\dot{m}_{leak}$ to the exhaust pressure with an adiabatic mixing between the flow rates $\dot{m}_{in}$ and $\dot{m}_{leak}$ (ex,2 → ex,1),
- an isobaric exhaust cooling down or heating up (ex,1 → ex).

The mass flow rate swept by the expander is a function of the expander swept volume V_{sw}, the rotational speed N and the leakage flow rate:

$$\dot{m} = \dot{m}_{in} + \dot{m}_{leak} = \frac{V_{sw} \cdot N}{v_{su,2}} + \dot{m}_{leak} \tag{1}$$

All of the leakage paths are lumped into one unique fictitious leakage path connecting the expander intake and exhaust. The leakage flow rate as well as the pressure drop at the expander inlet are simulated by reference to the isentropic flows through simply convergent nozzles with cross-sectional areas A_{leak} and A_{su},

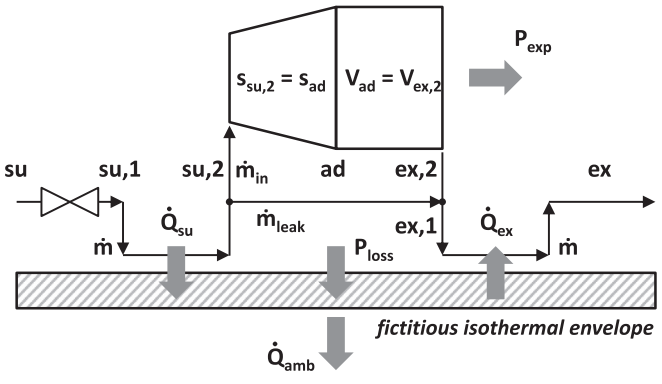

Fig. 1. Schematic representation of the expander simulation model.

respectively.

The model includes under- and over-expansion losses by splitting the expansion into an isentropic process and a constant-volume evolution, as anticipated, leading to the following expression for the internal expansion power

$$P_{in} = \dot{m}_{in} \cdot \left[(h_{su,2} - h_{ad}) + v_{ad} \cdot \left(p_{ad} - p_{ex,2} \right) \right] \quad (2)$$

where the adapted condition is calculated by $v_{ad} = BVR \cdot v_{su,2}$ and $s_{ad} = s_{su,2}$.

The model takes into account both mechanical losses ($P_{loss,mec}$) due to friction between the moving elements (scrolls, journal bearings, Oldham coupling, etc.) and electromechanical losses ($P_{loss,ele}$) in the asynchronous machine:

$$P_{exp} = P_{in} - P_{loss,mec} - P_{loss,ele} \quad (3)$$

Mechanical losses are simulated by introducing the mechanical efficiency:

$$P_{loss,mec} = (1 - \eta_{mec}) \cdot P_{in} \quad (4)$$

Electromechanical losses are evaluated on the basis of the performance of the asynchronous machine in motor mode and expressed as a function of the shaft rotational speed [24].

$$P_{loss,ele} = 199 - 0.4553 \cdot (3002 - N) + 0.03699 \cdot (3002 - N)^2 \quad (5)$$

The rotational speed of the expander increases slightly with the power it produces, as a result of the speed sliding characteristic of the asynchronous machine. The following relationship has been derived from the performance given by the manufacturer of the asynchronous machine [24].

$$N = 3007 - 0.02155 \cdot P_{exp} + 0.000002091 \cdot P_{exp}^2 \quad (6)$$

Internal heat transfers are lumped into equivalent supply $\dot{Q}_{su}$ and exhaust $\dot{Q}_{ex}$ heat transfer rates between the fluid and a fictitious shell of uniform temperature T_{sh}, by introducing the overall heat transfer coefficients AU_{su} and AU_{ex}. In detail, the supply heat transfer rate is calculated as

$$\dot{Q}_{su} = \dot{m} \cdot (h_{su,1} - h_{su,2}) = \left(1 - e^{\frac{-AU_{su}}{\dot{m} \cdot c_p}} \right) \cdot \dot{m} \cdot c_p \cdot (T_{su,1} - T_{sh}) \quad (7)$$

A similar formulation is adopted for the exhaust heat transfer rate, whereas the external heat loss $\dot{Q}_{amb}$ is calculated by an overall heat transfer coefficient AU_{amb}. In steady state regime, the shell temperature is given by

$$\dot{Q}_{su} \pm \dot{Q}_{ex} - AU_{amb} \cdot (T_{sh} - T_{amb}) + P_{loss,mec} + P_{loss,ele} = 0 \quad (8)$$

The input variables of the expander simulation model are the supply and exhaust pressures and the supply temperature. The main output variables are the mass flow rate displaced by the expander, its electrical power production and the exhaust temperature. As listed in Table 1, the model needs eight parameters, which are tuned in order to best match the values of the output variables with the measurements [24].

Although a more physically sound modelling can be proposed as regards mechanical [27,28] and ambient heat losses [27–30], the model adopted by Lemort et al. [24] is reliable with a maximum deviation between the prediction and the measurements of 2% for the mass flow rate, 6% for the power output, and 2 K for the exhaust temperature. In addition, the applicability of the model is sufficiently wide as regards the ranges of fluid pressure at the expander inlet (from 2 to 35 bar) and pressure ratio (from 2 to 20) [24].

2.2. The change of the working fluid

A reasonable assessment of the performance of the scroll expander in case of working fluids other than R245fa is possible based on the procedure originally proposed in a former work [25]. In detail, considering the geometry of the expander is definitively fixed, only heat transfer coefficients should be varied when changing the working fluid. Lemort et al. [24] introduced eq. (7) to simulate both supply and exhaust heat transfer rates and the following formula

$$AU_{su} = AU_{ex} = 30 \cdot \left(\frac{\dot{m}}{0.1} \right)^{0.6} \quad (9)$$

was used for calculating the heat transfer coefficients (Table 1), where $\dot{m}$ and 0.1 (kg/s) are the mass flow rate and a reference value for normalization, respectively. Thus, based on the consideration that orifices, flow passage areas and the general geometry of the scroll expander do not vary when changing the working fluid:

$$AU \propto \frac{Nu \cdot \lambda}{L} \propto Re^x \cdot Pr^y \cdot \lambda \quad (10)$$

where $Re^x \cdot Pr^y$ is introduced in place of the Nusselt number. Ultimately, the supply and exhaust heat transfer coefficients in Table 1 have been revised according to the specific working fluid [25], by leaving intact the original semi-empirical structure modelling the expander.

2.3. Calculation tools and working fluids

The scroll expander model has been implemented in the MATLAB® environment. As anticipated in sections 2.1 and 2.2, some model equations need the fluid thermodynamic and transport properties, so use of the REFPROP database, as developed by the National Institute of Standards and Technology of the United States [31], has been made.

The REFPROP database includes seven fourth-generation refrigerants, whose main thermo-physical and environmental properties are detailed in Table 2, along with the ones of R245fa for comparison. The parameter of molecular complexity σ is also reported, defined as [32]:

$$\sigma = \frac{T_{cr}}{R} \cdot \left(\frac{\partial s}{\partial T} \right)_{sv, T_r = 0.7} \quad (11)$$

which is related to the slope of the saturated vapor line: the more positive σ, the more complex the molecular structure. In particular, fluids with positive values of σ superheat themselves during an isentropic expansion, with a reduced temperature drop as σ increases.

Fig. 2 shows the relation between pressure and temperature at saturation conditions of all the fluids considered in this work, whereas Fig. 3 shows five T-s diagrams, after excluding the fluids whose curves in Fig. 2 have steeper slopes.

As detailed in Table 2, the fourth-generation refrigerants have a really lower GWP compared to R245fa [10,33]. In particular, as GWP is a function, among other properties, of the atmospheric lifetime (ALT), lower ALT reflects on lower GWP. On the other hand, among the low-GWP fluids in Table 2, there are two hydrochlorofluoroolefins (HCFOs), namely R1224yd(Z) and R1233zd(E). The presence of chlorine in the molecule does reflect on a non-zero ODP, even though it is very negligible [33].

Table 1
Parameters of the scroll expander simulation model [24].

parameter	description	value	units
A_{leak}	leakage cross-sectional area (p_{su} in bar)	$0.68 - 0.116 \cdot (10 - p_{su})$	mm^2
A_{su}	inlet port cross-sectional area	30	mm^2
AU_{su}	supply heat transfer coefficient ($\dot{m}$ in $kg \cdot s^{-1}$)	$30 \cdot \left(\frac{\dot{m}}{0.1}\right)^{0.6}$	$W \cdot K^{-1}$
AU_{ex}	exhaust heat transfer coefficient ($\dot{m}$ in $kg \cdot s^{-1}$)	$30 \cdot \left(\frac{\dot{m}}{0.1}\right)^{0.6}$	$W \cdot K^{-1}$
AU_{amb}	ambient heat transfer coefficient	3.4	$W \cdot K^{-1}$
BVR	built-in volume ratio	2.85	–
V_{sw}	swept volume	22.4	cm^3
η_{mec}	mechanical efficiency	0.9	–

Table 2
Main thermo-physical [31] and environmental [10,33] properties of the fluids considered in this work.

	R245fa	R1234yf	R1234ze(E)	R1234ze(Z)	R1243zf	R1336mzz(Z)	R1224yd(Z)	R1233zd(E)
Molecular formula	$CHF_2CH_2CF_3$	$CF_3CF{=}CH_2$	$CF_3CH{=}CHF$	$CF_3CH{=}CHF$	$CF_3CH{=}CH_2$	$CF_3CH{=}CHCF_3$	$CF_3CF{=}CHCl$	$CF_3CH{=}CHCl$
Molecular mass, kg/kmol	134.05	114.04	114.04	114.04	96.05	164.06	148.49	130.5
Critical temperature, °C	153.86	94.7	109.36	150.12	103.78	171.27	155.54	166.45
Critical pressure, bar boiling point, °C	36.51	33.82	36.35	35.31	35.18	29.03	33.37	36.24
Latent heat at boiling point, kJ/kg	15.05	−29.49	−18.97	9.73	−25.42	33.38	14.62	18.26
Equation of state in REFPROP	196.77 [31,34]	180.25 [31,35]	195.62 [31,36]	215.12 [31,37]	217.18 [31,37]	165 [31,38]	168.87 [31,39]	194.62 [31,40]
Molecular complexity σ	2.41	−0.17	−0.23	−0.73	−1.85	5.99	2.69	1.79
ODP	0	0	0	0	0	0	0.00012	0.00034
GWP	858	<1	<1	<1	<1	2	<1	1
ALT, days	2811[a)]	10.5	16.4	10	7	22	21	26

[a] 7 years.

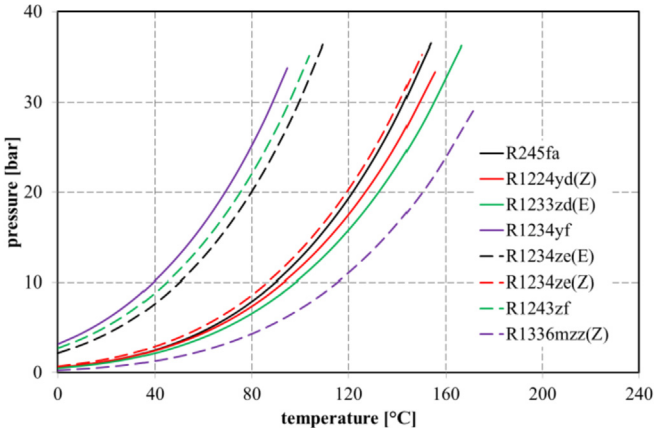

Fig. 2. Vapor pressure curves for the fluids considered in this work.

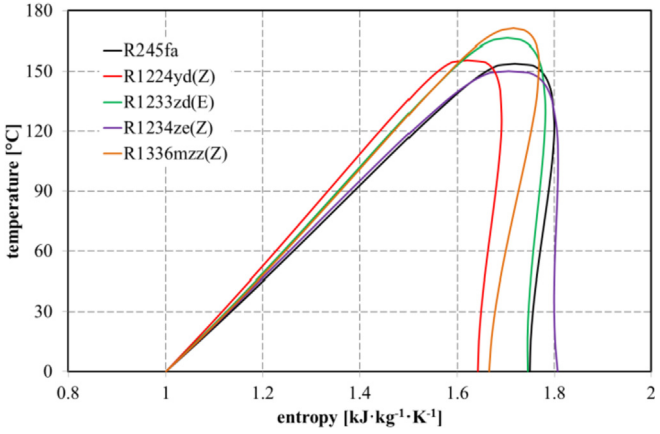

Fig. 3. T-s diagrams of R245fa and four selected low-GWP fluids.

3. Results and discussion

As anticipated in section 2, after setting the supply temperature and the supply and exhaust pressures as the input variables of the expander model, it is possible to simulate the behavior of the scroll expander. The results of the performance of the scroll expander are reported in this section, based on calculations of micro ORC systems (see Fig. 4) simulated according to few basic assumptions: (i) the fluid condensation temperature is set at 40 °C (unless specified otherwise), without liquid subcooling, (ii) the pressure losses in both evaporator and condenser are neglected and (iii) the overall efficiency of the pump is set at 0.5. This value is reasonable based on recent experimental researches on diaphragm [41] and gear pumps [42], since maximum values in the ranges 45–48% and 50–60% respectively have been demonstrated.

3.1. Cases with R245fa

Lemort et al. [24] validated their original model for a certain degree of R245fa superheating at the expander inlet. Here, three degrees of R245fa superheating at the expander inlet are preliminarily considered. Fig. 5 shows the cycle efficiency

$$\eta_{ORC} = \frac{P_{exp} - P_{pump}}{\dot{Q}_{input}} \tag{12}$$

in case of electric power output of the expander from 1 to 2 kW, with steps of 0.1 kW. Eq. (12) considers net electricity production (P_{pump} is the overall pump consumption and $\dot{Q}_{input}$ is the heat input for fluid economizing, evaporating and superheating). Based on the calculation assumptions, higher pressure ratio, reflecting on higher fluid temperature at the expander inlet, is required for higher

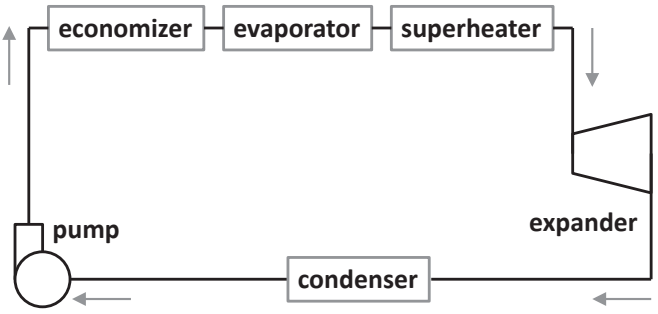

Fig. 4. ORC layout with main components.

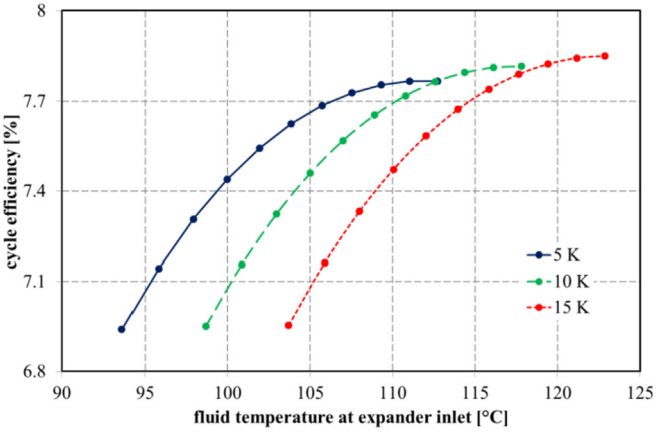

Fig. 5. Cycle efficiency as a function of R245fa temperature at the expander inlet for three degrees of fluid superheating (condenser temperature fixed at 40 °C). The elec-tric power output of the expander ranges from 1 to 2 kW.

power output from the expander. Fig. 5 also shows that the cycle efficiency is shifted to the right for higher degrees of fluid superheating, without significant variations. As a matter of fact, very slight improvements can be appreciated only for higher power outputs. According to this first result, 5 K may be selected as the fluid superheating for a heat source with a temperature as low as possible [43], even though the degree of fluid superheating at the evaporator outlet may affect the operation stability of the micro ORC system [44].

Paying attention to the results strictly related to the expander behavior, Fig. 6 shows the output power curves for the three degrees of fluid superheating, which are almost superimposed, so the pressure ratio is the main variable for the desired power output of the expander, with a clearly linear trend. As regards the supply volumetric flow rate, it is possible to appreciate the little influence of the degree of fluid superheating as well as a slight variation in spite of an almost constant value of the rotational speed as resulting from Eq. (6) for the considered range of power outputs. In detail, the increasing trend with the fluid pressure at the expander inlet is justified by referring to Eq. (1), as the higher the pressure the larger the leakage flow rate.

The linear trend of the power output with the fluid pressure at the expander inlet is also achieved in case of lower condenser temperatures, as reported in Fig. 7, where three equal slopes can be appreciated. This result does depend on the almost constant rotational speed (the higher the rotational speed, the steeper the slope) and is not unusual for positive-displacement expanders [28].

Based on this last result, Fig. 8 shows the cycle efficiency calculated in case of three condenser temperatures for gross

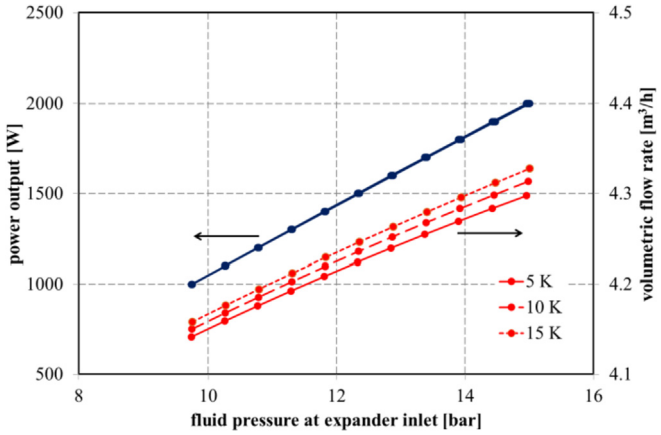

Fig. 6. Power output from the expander and supply volumetric flow rate as functions of R245fa pressure at the expander inlet for three degrees of fluid superheating (condenser temperature fixed at 40 °C).

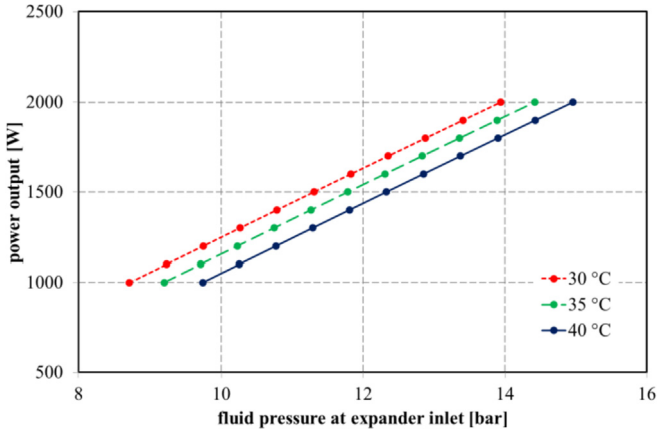

Fig. 7. Power output from the expander as a function of R245fa pressure at the expander inlet (fluid superheating set at 5 K) for three condenser temperatures.

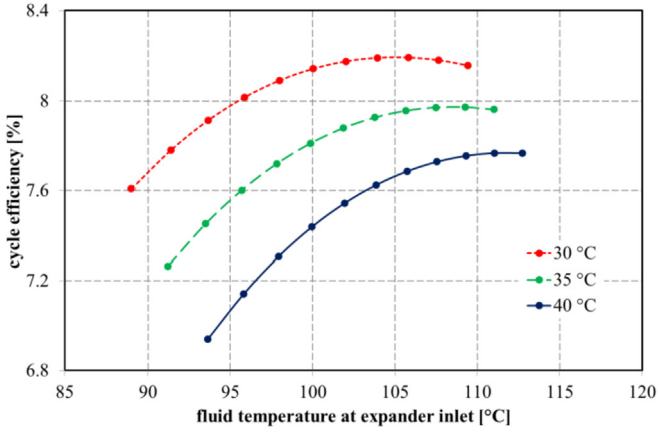

Fig. 8. Cycle efficiency as a function of R245fa temperature at the expander inlet (fluid superheating set at 5 K) for three condenser temperatures. The electric power output of the expander ranges from 1 to 2 kW.

electric power outputs in the range from 1 to 2 kW. Although a condenser temperature of 40 °C is a conservative hypothesis for micro ORC systems [43], a better performance seems to be possible for lower condenser temperatures.

3.2. Cases with HFOs and HCFOs

Based on the results achieved with R245fa, in order to propose a fair comparison, the fluid superheating at the expander inlet is always set at 5 K for the analysis with HFOs and HCFOs.

Focusing on two power outputs from the expander (1 and 2 kW) for the sake of simplicity, Fig. 9 reports both the cycle efficiency and the corresponding fluid temperature at the expander inlet for a condenser temperature fixed at 40 °C. The results of the seven low-GWP fluids are compared to the ones of R245fa and suggest the following indications.

- R1234yf, R1243zf and R1234ze(E) require a lower fluid temperature at the expander inlet compared to R245fa and the cycle efficiency is lower as well. Considering that R1234yf and R1234ze(E) are suggested as substitute fluids for R134a in ORC systems [45], this result is consistent with the ones achieved by other researchers in case of operation with R134a instead of R245fa [5–9].
- Although it is not commercialized in refrigerant quality, R1234ze(Z) seems to be a serious low-GWP alternative to R245fa. As a matter of fact, the calculations return almost equal fluid temperatures at the expander inlet for the same performance.
- Slightly higher fluid temperatures at the expander inlet are necessary in case of operation with the two HCFOs, namely R1224yd(Z) and R1233zd(E), with a modest improvement of the cycle efficiency.

Limited to the last three fluids and including also R1336mzz(Z), Fig. 10 reports the cycle efficiency as a function of the fluid temperature at the expander inlet for an electric power output of the expander ranging from 1 to 2 kW, similarly to Fig. 5 for R245fa. Fig. 10 highlights a behavior with R1336mzz(Z) which is different when compared to the ones of the other three fluids and almost the same efficiency is achieved in case of 1 and 2 kW of power output from the expander (as anticipated in Fig. 9). In addition, around 17 and 21 K more than the fluid temperature at the expander inlet required for R245fa are necessary for power outputs from the expander of 1 and 2 kW, respectively. Thus, R1336mzz(Z) does not seem to be as adequate as R1234ze(Z), R1224yd(Z) and R1233zd(E) to replace R245fa for the considered application with the scroll expander investigated here.

The results in Fig. 10 can be better justified by referring to the

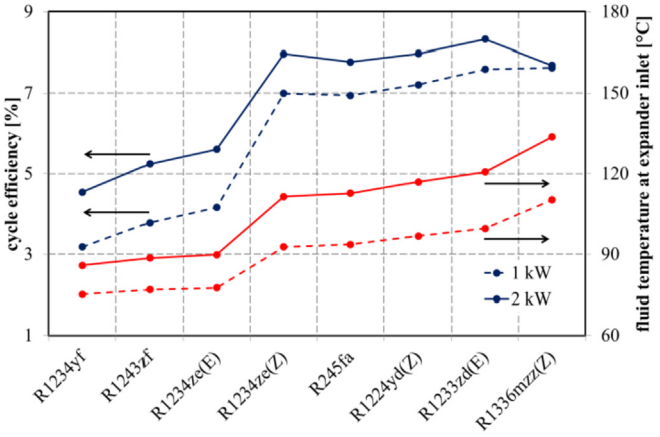

Fig. 9. Cycle efficiency and corresponding fluid temperature at the expander inlet (fluid superheating set at 5 K) for expander power outputs of 1 and 2 kW (condenser temperature fixed at 40 °C).

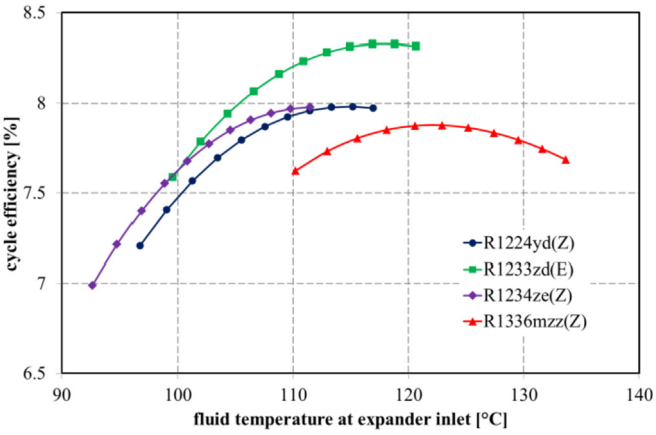

Fig. 10. Cycle efficiency as a function of the fluid temperature at the expander inlet (fluid superheating set at 5 K). The electric power output of the expander ranges from 1 to 2 kW (condenser temperature fixed at 40 °C).

expander efficiency. In particular, higher cycle maximum temperature does not reflect on higher cycle efficiency because of the actual value of the expander efficiency:

$$\eta_{exp} = \frac{P_{exp}}{\dot{m} \cdot (h_{su} - h_{ex,is})} \tag{13}$$

where the isentropic condition at the denominator is calculated by $p_{ex,is} = p_{ex}$ and $s_{ex,is} = s_{su}$. The expander efficiency reported in Fig. 11 is not constant and does depend on the pressure ratio [46]. As a matter of fact, the higher the pressure ratio, the lower the expander efficiency as the result of a larger under-expansion.

Similarly to the case with R245fa, Fig. 12 reports a linear trend between the power output from the expander and the fluid pressure at the expander inlet. Once again, the slope is constant and does not depend on the specific working fluid. The more the saturation pressure curve is shifted to the right, towards higher temperatures (see Fig. 2), the lower the supply pressure required for a fixed power output.

3.3. Cases with mixtures of HFOs

As shown in Fig. 9, different fluid temperatures at the expander inlet are necessary for a specific power output from the expander, depending on the selected working fluid. Compared to the case

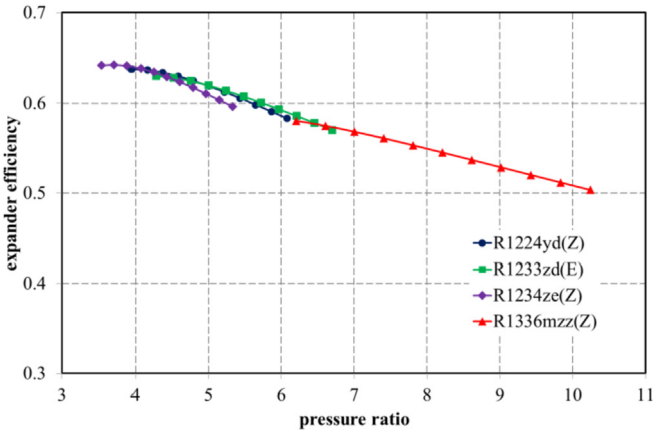

Fig. 11. Expander efficiency vs. pressure ratio for the cases reported in Fig. 10.

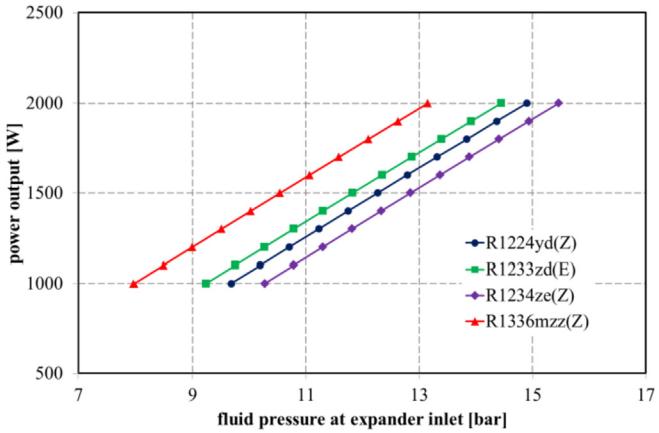

Fig. 12. Power output from the expander as a function of the fluid pressure at the expander inlet (condenser temperature fixed at 40 °C).

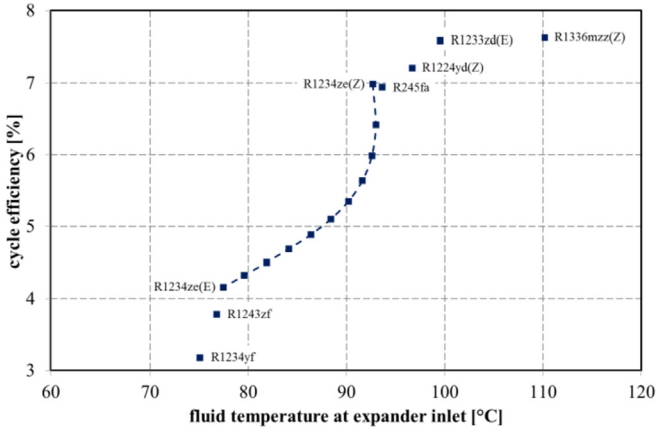

Fig. 13. Cycle efficiency and corresponding fluid temperature at the expander inlet (fluid superheating set at 5 K) for 1 kW of expander power output (condenser tem-perature fixed at 40 °C).

with R245fa, an almost equal temperature is required for 2 kW of gross power output with R1234ze(Z), i.e. 111.5 °C instead of 112.7 °C, but slightly higher temperatures are necessary in case of R1224yd(Z) or R1233zd(E), i.e. 116.9 °C or 120.7 °C, respectively. When exploiting lower temperature heat sources, Fig. 9 suggests R1234ze(E) with 89.8 °C as fluid temperature at the expander inlet, but the temperature gap is significant when passing from R1234ze(Z) to R1234ze(E), and vice versa. In order to bridge this temperature gap, a binary mixture could be proposed.

Based on the previous calculation assumptions, Figs. 13 and 14 propose the results of the cycle efficiency as a function of the fluid temperature at the expander inlet for R245fa and the seven considered low-GWP fluids in the cases of 1 and 2 kW of power output from the expander, respectively. In addition, a number of points in both the figures are representative of nine mixtures of R1234ze(E) and R1234ze(Z), with a 10 to 90 wt% content of the first substance compared to the second in the pair (with a fixed step of 10 wt%).[2] Of course, the performance of each fluid or mixture moves up and to the right in case of higher power output from the

[2] These results should be considered as a preliminary assessment of performance trends, since no mixture data are available in the REFPROP database for the binary pair of R1234ze(E) and R1234ze(Z) and the mixing parameters have been estimated by default [31].

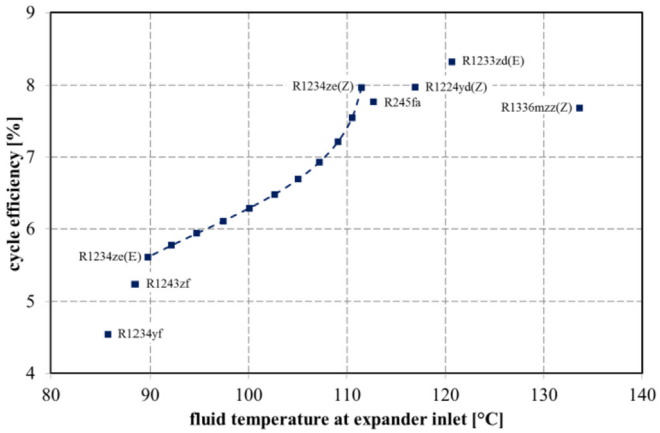

Fig. 14. Cycle efficiency and corresponding fluid temperature at the expander inlet (fluid superheating set at 5 K) for 2 kW of expander power output (condenser temperature fixed at 40 °C).

expander. As anticipated in Fig. 9, the points characteristic of R1234ze(Z) and R245fa are very close to each other, whereas mixing R1234ze(E) and R1234ze(Z) seems to be an effective solution to bridge the temperature gap in both Figs. 13 and 14 between these two fluids.

3.4. Remarks about the pump

The results of the cycle efficiency presented in the previous sections depend on the calculation assumptions and, in particular, on the overall efficiency of the pump. Although the extent of research on expanders for low power applications (below 10 kW) is large, the literature about the pump is limited. Among the various types, diaphragm pumps seem to be the most favored for low power output ORCs. Manufacturers claim efficiency values generally higher than 40–50%, even though Quoilin et al. [47] reported that these values are rarely achieved in reality, with efficiency values typically in the range 7–33%. On the other hand, recent researches on the actual performance of diaphragm [41] and gear pumps [42] for low power output ORCs have reported a maximum overall efficiency of these pumps in the ranges 45–48% and 50–60%, respectively.

Focusing on the ORC calculations for an expander power output of 2 kW, Table 3 details the results concerning the pump for the eight fluids in Table 2 and Fig. 9. Once again, with the exception of

Table 3
Calculation results for the ORC pump in case of 2 kW of expander power output.

	Q_{pump}, cm^3/s	Δp_{pump}, bar	P_{pump}, W	μ, cP[a)]
R245fa	78	12.5	193	0.33
R1234yf	197	15.4	607	0.13
R1234ze(E)	143	14.6	415	0.16
R1234ze(Z)	80	12.6	201	0.26
R1243zf	164	14.8	486	0.13
R1336mzz(Z)	78	11.9	185	0.32
R1224yd(Z)	84	12.4	210	0.27
R1233zd(E)	76	12.3	187	0.25

[a)] 1 cP = 10^{-3} Pa·s.

the fluids whose curves in Fig. 2 have steeper slopes, namely R1234yf, R1243zf and R1234ze(E), the results for the other five fluids are almost similar, suggesting that replacing R245fa with the other fluids is quite reasonable. In particular, the volumetric flow

rate (Q_{pump}) gives an idea of the size of the pump, in case of adopting a positive-displacement machine.

The last column on the right in Table 3 details the fluid viscosity at pump suction conditions (40 °C). These values are reported for further considerations about the efficiency of the pump when changing the working fluid. As a matter of fact, even based on simple theories of positive-displacement pumps [48–50], volumetric losses are dependent on the ratio between the pressure drop across the pump and the fluid viscosity ($\Delta p/\mu$). On the other hand, hydraulic-mechanical losses due to viscous friction between the sliding surfaces of the machine directly depend on fluid viscosity. Compared to the case with R245fa, lower fluid viscosity should reflect on lower volumetric efficiency but higher hydraulic-mechanical efficiency. Thus, as a first approximation, the overall pump efficiency could be considered unchanged.

4. Conclusions

A model reported in literature [24] for simulating the performance of a 2 kW hermetic scroll expander has been revised and used to study the behavior of the machine in case of replacing the original high-GWP working fluid (R245fa) with fourth-generation refrigerants, i.e. low-GWP fluids.

Calculations of micro ORC systems with the selected expander have resulted in almost equal performance of R1234ze(Z) compared to R245fa and even slightly better performance when using R1224yd(Z) or R1233zd(E), but with a modest increase of the fluid temperature at the expander inlet. In particular, the results with R1336mzz(Z) do not seem to be as interesting as the ones with the previous three low-GWP fluids. In case of lower heat sources, R1234yf, R1243zf and R1234ze(E) are possible working fluids and mixtures of HFOs could be also considered to extend the operation range of the expander. However, the lower the fluid temperature at the expander inlet, the lower the cycle efficiency for a fixed expander power output. Details about the pump consumptions are reported as well along with some considerations about the vis-cosity of the fluid affecting both volumetric and hydraulic-mechanical losses.

These conclusions result from thermodynamic calculations with low-GWP working fluids, but further considerations about chemical stability, safety, etc., are obviously necessary for a proper selection of the working fluid. According to the HFO-related literature, the maximum temperatures calculated in this work should not raise concerns about chemical stability. In addition, the considered fourth-generation refrigerants are class A fluids as regards the toxicity, whereas R245fa is a class B fluid. On the other hand, R1224yd(Z), R1233zd(E) and R1336mzz(Z) are non-flammable fluids, as well as R245fa, but the other four low-GWP fluids are mildly flammable and release hazardous substances such as hydrogen fluoride in case of burning.

Nomenclature

A	area, m^2
ALT	atmospheric lifetime
AU	heat transfer coefficient, $W \cdot K^{-1}$
BVR	built-in volume ratio
c_p	specific heat at constant pressure, $J \cdot kg^{-1} \cdot K^{-1}$
CFC	chlorofluorocarbon
GWP	global warming potential
h	specific enthalpy, $J \cdot kg^{-1}$
HCFC	hydrochlorofluorocarbon
HCFO	hydrochlorofluoroolefin
HFC	hydrofluorocarbon
HFO	hydrofluoroolefin
L	length, m
$\dot{m}$	mass flow rate, $kg \cdot s^{-1}$
N	rotational speed, rpm
Nu	Nusselt number
ODP	Ozone depletion potential
ORC	organic Rankine cycle
p	pressure, Pa
P	power, W
Pr	Prandtl number
Q	volumetric flow rate, $m^3 \cdot s^{-1}$
$\dot{Q}$	heat transfer rate, W
R	gas constant, $J \cdot kg^{-1} \cdot K^{-1}$
Re	Reynolds number
S	specific entropy, $J \cdot kg^{-1} \cdot K^{-1}$
T	temperature, K
U	thermal transmittance, $W \cdot m^{-2} \cdot K^{-1}$
v	specific volume, $m^3 \cdot kg^{-1}$
V	volume, m^3
η	efficiency
λ	thermal conductivity, $W \cdot m^{-1} \cdot K^{-1}$
μ	viscosity, $Pa \cdot s$
σ	molecular complexity
Δ	difference

Subscripts

ad	adapted
amb	ambient
cr	critical
ele	electric
ex	exhaust
exp	expander
in	internal
is	isentropic
leak	leakage
loss	loss
mec	mechanical
pump	pump
r	reduced
sh	shell
su	supply
sv	saturated vapour
sw	swept

References

[1] Colonna P, Casati E, Trapp C, Mathijssen T, Larjola J, Turunen-Saaresti T, Uusitalo A. Organic Rankine cycle power systems: from the concept to current technology, applications, and an outlook to the future. J Eng Gas Turbines Power 2015;137(10). 100801.

[2] Saleh B, Koglbauer G, Wendland M, Fischer J. Working fluids for low-temperature organic Rankine cycles. Energy 2007;32(7):1210–21.

[3] Chen H, Goswami DY, Stefanakos EK. A review of thermodynamic cycles and working fluids for the conversion of low-grade heat. Renew Sustain Energy Rev 2010;14(9):3059–67.

[4] Quoilin S, Van Den Broek M, Declaye S, Dewallef P, Lemort V. Techno-economic survey of organic Rankine cycle (ORC) systems. Renew Sustain Energy Rev 2013;22:168–86.

[5] Song P, Wei M, Shi L, Danish SN, Ma C. A review of scroll expanders for organic Rankine cycle systems. Appl Therm Eng 2015;75:54–64.

[6] Imran M, Usman M, Park BS, Lee DH. Volumetric expanders for low grade heat and waste heat recovery applications. Renew Sustain Energy Rev 2016;57:1090–109.

[7] Zywica G, Kaczmarczyk TZ, Ihnatowicz E. A review of expanders for power generation in small-scale organic Rankine cycle systems: performance and operational aspects. Proc IME J Power Energy 2016;230(7):669–84.

[8] Rahbar K, Mahmoud S, Al-Dadah RK, Moazami N, Mirhadizadeh SA. Review of organic Rankine cycle for small-scale applications. Energy Convers Manag 2017;134:135–55.

[9] Bao J, Zhao L. A review of working fluid and expander selections for organic

Rankine cycle. Renew Sustain Energy Rev 2013;24:325–42.
[10] Myhre G, Shindell D, Bréon FM, Collins W, Fuglestvedt J, Huang J, Koch D, Lamarque JF, Lee D, Mendoza B, Nakajima T, Robock A, Stephens G, Takemura T, Zhang H. Anthropogenic and Natural Radiative Forcing, In: Climate Change 2013: The Physical Science Basis. Contribution of Working Group I to the Fifth Assessment Report of the Intergovernmental Panel on Climate Change, available at: https://www.ipcc.ch/pdf/assessment-report/ar5/wg1/WG1AR5_Chapter08_FINAL.pdf, last access on December 20, 2017.
[11] Jarall S. Study of refrigeration system with HFO-1234yf as a working fluid. Int J Refrig 2012;35(6):1668–77.
[12] Navarro-Esbri J, Mendoza-Miranda JM, Mota-Babiloni A, Barragan-Cervera A, Belman-Flores JM. Experimental analysis of R1234yf as a drop-in replacement for R134a in a vapour compression system. Int J Refrig 2013;36:870–80.
[13] Fukuda S, Kondou C, Takata N, Koyama S. Low GWP refrigerants R1234ze(E) and R1234ze(Z) for high temperature heat pumps. Int J Refrig 2014;40: 161–73.
[14] Liu W, Meinel D, Wieland C, Spliethoff H. Investigation of hydrofluoroolefins as potential working fluids in organic Rankine cycle for geothermal power generation. Energy 2014;67:106–16.
[15] Le VL, Feidt M, Kheiri A, Pelloux-Prayer S. Performance optimization of low-temperature power generation by supercritical ORCs (organic Rankine cy-cles) using low GWP (global warming potential) working fluids. Energy 2014;67:513–26.
[16] Yamada N, Mohamed MNA, Trung KT. Study on thermal efficiency of low to medium temperature organic Rankine cycles using HFO-1234yf. Renew Energy 2012;41:368–75.
[17] Petr P, Raabe G. Evaluation of R-1234ze(Z) as drop-in replacement for R-245fa in Organic Rankine Cycles - from thermophysical properties to cycle performance. Energy 2015;93:266–74.
[18] Ziviani D, Dickes R, Quoilin S, Lemort V, De Paepe M, van den Broek M. Organic Rankine cycle modelling and the ORCmKit library: analysis of R1234ze(Z) as drop-in replacement of R245fa for low-grade waste heat recovery. In: Proceedings of ECOS; 2016. June 19-23, 2016, Portorož, Slovenia.
[19] Moles F, Navarro-Esbrí J, Peris B, Mota-Babiloni A, Barragan-Cervera A, Kontomaris K. Low GWP alternatives to HFC-245fa in Organic Rankine Cycles for low temperature heat recovery: HCFO-1233zd-E and HFO-1336mzz-Z. Appl Therm Eng 2014;71:204–12.
[20] Molés F, Navarro-Esbrí J, Peris B, Mota-Babiloni A. Experimental evaluation of HCFO-1233zd-E as HFC-245fa replacement in an Organic Rankine Cycle system for low temperature heat sources. Appl Therm Eng 2016;98:954–61.
[21] Navarro-Esbrí J, Molés F, Peris B, Mota-Babiloni A, Kontomaris K. Experimental study of an Organic Rankine Cycle with HFO-1336mzz-Z as a low global warming potential working fluid for micro-scale low temperature applications. Energy 2017;133:79–89.
[22] Eyerer S, Wieland C, Vandersickel A, Spliethoff H. Experimental study of an ORC (Organic Rankine Cycle) and analysis of R1233zd-E as a drop-in replacement for R245fa for low temperature heat utilization. Energy 2016;103:660–71.
[23] Giuffrida A, Pezzuto D. Simulation of a scroll expander using R1233zd(E), R1234ze(Z) and their mixtures as drop-in replacements for R245fa. Energy Procedia 2017;129:301–6.
[24] Lemort V, Declaye S, Quoilin S. Experimental characterization of a hermetic scroll expander for use in a micro-scale Rankine cycle. Proc IME J Power Energy 2012;226(1):126–36.
[25] Giuffrida A. Modelling the performance of a scroll expander for small organic Rankine cycles when changing the working fluid. Appl Therm Eng 2014;70: 1040–9.
[26] Lemort V. Contribution to the characterization of scroll machines in compressor and expander modes. PhD thesis. University of Liege; 2008. available at:, http://bictel.ulg.ac.be/ETD-db/collection/available/ULgetd-03302009-081543/unrestricted/PhD_VLemort2008.pdf.
[27] Giuffrida A. A semi-empirical method for assessing the performance of an open-drive screw refrigeration compressor. Appl Therm Eng 2016;93: 813–23.
[28] Giuffrida A. Improving the semi-empirical modelling of a single-screw expander for small organic Rankine cycles. Appl Energy 2017;193:356–68.
[29] Dardenne L, Fraccari E, Maggioni A, Molinaroli L, Proserpio L, Winandy E. Semi-empirical modelling of a variable speed scroll compressor with vapour injection. Int J Refrig 2015;54:76–87.
[30] Molinaroli L, Joppolo CM, De Antonellis S. A semi-empirical model for hermetic rolling piston compressors. Int J Refrig 2017;79:226–37.
[31] www.nist.gov/srd/refprop, last access on December 20, 2017.
[32] Invernizzi C, Iora P, Silva P. Bottoming micro-Rankine cycles for micro-gas turbines. Appl Therm Eng 2007;27(1):100–10.
[33] www.coolingpost.com/world-news/new-hcfo-refrigerant-ashrae-listed, last access on December 20, 2017.
[34] Akasaka R, Zhou Y, Lemmon EW. A fundamental equation of state for 1,1,1,3,3-pentafluoropropane (R-245fa). J Phys Chem Ref Data 2015;44(1): 1–11.
[35] Richter M, McLinden MO, Lemmon EW. Thermodynamic properties of 2,3,3,3-Tetrafluoroprop-1-ene (R1234yf): vapor pressure and p-rho-T measurements and an equation of state. J Chem Eng Data 2011;56(7):3254–64.
[36] Thol M, Lemmon EW. Equation of state for the thermodynamic properties of trans-1,3,3,3-tetrafluoropropene [R1234ze(E)]. Int J Thermophys 2016;37:28.
[37] Akasaka R, Lemmon EW. Fundamental Equations of State for cis-1,3,3,3-Tetrafluoropropene (R-1234ze(Z)) and 3,3,3-Trifluoropropene (R-1243zf). J Chem Eng Data 2018.
[38] Akasaka R, Lemmon EWA. Helmholtz energy equation of state for cis-1,1,1,4,4,4-hexafluoro-2-butene (R-1336mzz(Z)). In: The 8th Asian conference on refrigeration and air-conditioning; May 15-17, 2016 [Taipei, Taiwan].
[39] Akasaka R, Fukushima M, Lemmon EW. A Helmholtz energy equation of state for Cis-1-chloro-2,3,3,3-tetrafluoropropene (R-1224yd(Z)), European conference on thermophysical properties. September 3-8, 2017 [Graz, Austria].
[40] Mondejar ME, McLinden MO, Lemmon EW. Thermodynamic properties of trans-1-chloro-3,3,3-trifluoropropene (R1233zd(E)): vapor pressure, p-rho-T data, speed of sound measurements and equation of state. J Chem Eng Data 2015;60:2477–89.
[41] Carraro G, Pallis P, bAris D, Leontaritis AD, Karellas S, Vourliotis P, Rech S, Lazzaretto A. Experimental performance evaluation of a multi-diaphragm pump of a micro-ORC system. Energy Procedia 2017;129:1018–25.
[42] Zeleny Z, Vodicka V, Novotny V, Mascuch J. Gear pump for low power output ORC – an efficiency analysis. Energy Procedia 2017;129:1002–9.
[43] Taccani R, Obi JB, De Lucia M, Micheli D, Toniato G. Development and experimental characterization of a small scale solar powered organic Rankine cycle (ORC). Energy Procedia 2016;101:504–11.
[44] Hu K, Zhu J, Zhang W, Liu K, Lu X. Effects of evaporator superheat on system operation stability of an organic Rankine cycle. Appl Therm Eng 2017;111: 793–801.
[45] Invernizzi CM, Iora P, Preßinger M, Manzolini G. HFOs as substitute for R-134a as working fluids in ORC power plants: a thermodynamic assessment and thermal stability analysis. Appl Therm Eng 2016;103:790–7.
[46] Declaye S, Quoilin S, Guillaume L, Lemort V. Experimental study on an open-drive scroll expander integrated into an ORC (Organic Rankine Cycle) system with R245fa as working fluid. Energy 2013;55:173–83.
[47] Quoilin S, Van Den Broek M, Declaye S, Dewallef P, Lemort V. Techno-economic survey of organic Rankine cycle (ORC) systems. Renew Sustain Energy Rev 2012;22:168–86.
[48] Wilson WE. Rotary pump theory. Trans. ASME 1946;68(4):371–84.
[49] Wilson WE. Performance criteria for positive-displacement pumps and fluid motors. Trans. ASME 1949;71(2):115–20.
[50] Ivantysyn J, Ivantysynova M. Hydrostatic pumps and motors. New Delhi, India: Technip Books International; 2003.